Int. J. Electrochem. Sci., 13 **(2018)** 209 – 224, doi: 10.20964/2018.01.03

International Journal of
ELECTROCHEMICAL
SCIENCE
www.electrochemsci.org

Mediated Electrochemical Oxidation of Pollutants in Crude Oil Desalter Effluent

F. García-Lugo[1,2], *A. Medel*[1,*], *J.L. Jurado Baizaval*[1], *P. Mijaylova Nacheva*[3], *A. Durán Moreno*[2], *M.J. Cruz Gómez*[2], *L. Godínez Mora-Tovar*[1] *and Y. Meas*[1,*]

[1] Centro de Investigación y Desarrollo Tecnológico en Electroquímica, S.C., Parque Tecnológico, Querétaro-Sanfandila, P.O. Box 064 – 76703, Pedro Escobedo, Querétaro, México.
[2] Facultad de Química, Universidad Nacional Autónoma de México, Col. Coyoacán- 04510 Ciudad de México, México.
[3] Instituto Mexicano de Tecnología del Agua, Blvd. Paseo Cuauhnáhuac 8532, Colonia Progreso – 62550 Jiutepec, Morelos, México.
[*]E-mail: yunnymeas@cideteq.mx, amedel@cideteq.mx

Received: 12 September 2017 / *Accepted:* 21 October 2017 / *Online Published:* 1 December 2017

Wastewater samples from a crude oil desalting process were subjected to extensive physicochemical characterization and electrolysis to evaluate the two main reaction pathways, electrochemical incineration and mediated oxidation, that occur during an electrochemical oxidation process (EOP) with a boron-doped diamond (BDD) anode. The effects of the main operating variables (pH, current density, and ionic composition) on the oxidation of organic pollutants and the production of hydroxyl radicals ($^{\bullet}$OH) were evaluated via spectroelectrochemistry, quantification of the total organic carbon (TOC), and fluorescence spectroscopy. The predominance of each reaction pathway was evaluated using tert-butyl alcohol (50 mM) as a $^{\bullet}$OH scavenger, the main oxidant species in electrochemical incineration. The results indicated that the action of $^{\bullet}$OH was minimal compared to that of active chlorine species (ClO^-, HClO, and Cl_2), oxychlorine radicals ($ClO^{\bullet}$, $ClO_2^{\bullet}$, $Cl^{\bullet}$, and $HOCl^{\bullet}$), and oxychlorine anion radicals ($Cl_2^{\bullet-}$, and $HOCl^{\bullet-}$). Under the optimal operating conditions (pH 8.5, j = 100 mA cm^{-2}, and t_r = 3 h), a 98.2% mineralization rate in terms of TOC was achieved. Mediated electrochemical oxidation was the predominant reaction pathway and was thus responsible for the high degradation efficiency obtained.

Keywords: desalter effluent; boron-doped diamond; electrochemical incineration; mediated electrochemical oxidation; active chlorine.

1. INTRODUCTION

Among the major liquid and highly toxic effluents generated in the various units of the petroleum refining process are those from tank bottom draws and sour water, spent lye, and desalter

effluent. The latter contains inorganic salts, sodium chloride, magnesium, and calcium [1], which must be removed to avoid the plugging and fouling of process equipment due to salt deposition and to reduce corrosion caused by the formation of HCl from chloride salts during the processing of the crude. To perform the desalting process, chemical [1], and electrostatic [2] processes are used; however, the water used can be contaminated with the different hydrocarbons contained in the drilling muds. In chemical treatments, chemical surfactants (demulsifiers) can also contribute to contamination. In both processes, contaminants such as ammonia, base or acid for pH adjustment can be introduced. The typical concentrations of cations in desalter effluent are 65,633, 8,350, 1,000, and 12.5 mg L^{-1} for Na^{+}, Ca^{2+}, Mg^{2+}, and Fe^{2+}, respectively. The concentrations of for anions are 118,925, 153, and 216 mg L^{-1} for Cl^{-}, HCO_3^{-}, and SO_4^{-2}, respectively [1]. Chemical oxygen demand (COD) values ranging from 345 to 12,000 mg L^{-1}, a total dissolved solids (TDS) level of 3,475.94 mg L^{-1}, and total hardness ($CaCO_3$) values ranging from 510.33 to 9,500 mg L^{-1} have been reported [3; 4]. Among the methods applied for the treatment of water from the crude oil desalting process are the use of American Petroleum Institute (API) separators, hydrocyclones [5], membrane distillation [1], ultrafiltration/reverse osmosis [3], and nanofiltration [4]. Crucially, the physicochemical composition of these effluents differs substantially from that of the produced water and caustic soda [6; 7]. During the literature review, no studies regarding the treatment of desalted water from crude oil refining using electrochemical processes — electrochemical oxidation using a boron-doped diamond (BDD) electrode in particular — were identified. The advantage of using a BDD electrode in wastewater treatment is its high capacity for $^{\bullet}OH$ production compared to any other material. This radical is the second strongest known oxidant after fluorine, with a high standard potential — $E°(^{\bullet}OH/H_2O)$ = 2.80 V vs. SHE at 25°C. The initial step in the electrochemical oxidation process (EOP) with BDD is the discharge of water molecules to form adsorbed hydroxyl radicals ($^{\bullet}OHs$) (Eq. 1). This reactive oxygen species can degrade toxic organic compounds into CO_2 and water (Eq. 2). This process is known as the electrochemical incineration process [8].

$$BDD + H_2O \rightarrow BDD\,(^{\bullet}OH) + H^{+} + e^{-} \quad \text{Eq. 1}$$

$$R + BDD\,(^{\bullet}OH) \rightarrow BDD + mCO_{2\,(g)} + nH_2O + H^{+} + e^{-} \quad \text{Eq. 2}$$

In Eq. 2, R is the fraction of a toxic organic compound containing no heteroatoms that needs one atom of oxygen to be transformed into fully oxidized products. The *m* and *n* values depend on the elemental composition of the compound to be oxidized. This reaction competes with the side reaction of $^{\bullet}OH$ discharge (either direct or indirect through the formation of H_2O_2 as an intermediate) to O_2 (Eq. 3) without any participation from the anode surface. BDD is considered a nonactive electrode.

$$BDD\,(^{\bullet}OH) \rightarrow BDD + 1/2O_{2\,(g)} + H^{+} + e^{-} \quad \text{Eq. 3}$$

BDD does not participate in the anodic reaction and does not provide any catalytically active site for the adsorption of reactants and/or products from the aqueous medium. Instead, it only serves as an inert substrate that acts as a sink for the removal of electrons. Outer sphere reactions (in which the reactant and product do not interact strongly with the electrode surface) and water discharge (as the

electrode is considered to be covered by at least one adsorbed layer of water molecules) are, in principle, the only possible anodic reactions for nonactive anodes [9]. Other characteristics of BDD are its high resistance to corrosion and its ability to generate additional oxidizing species (O_3 and H_2O_2) [10], in addition to its high over-potential for the oxygen evolution reaction (η–O_2) [11], which enables it to yield higher current efficiencies than other materials, such as Pt. The reactivity of BDD is governed by an outer sphere mechanism, but in the presence of chlorides and as a function of pH, this electrode can produce different active chloride oxidizing agents (ClO^-, HCl, and Cl_2), oxychlorine radicals ($ClO^{\bullet}$, $ClO_2^{\bullet}$, and $Cl^{\bullet}$), and oxychlorine anion radicals ($Cl_2^{\bullet-}$ and $ClOH^{\bullet-}$). The reaction mechanism is complicated and of great interest for pollutant destruction in wastewater. The process involving the participation of these species is called mediated electrochemical oxidation, [12] which, in the case of BDD, may also include the oxidation of additional anions, such as SO_4^{2-}, PO_4^{3-}, and CO_3^{2}, which would yield peroxodisulfate, peroxodiphosphate, and percarbonate, respectively (Eqs. 4–6) [13].

$$2SO_4^{2-} \rightarrow S_2O_8^{2-} + 2e^- \quad \text{Eq. 4}$$

$$2PO_4^{3-} \rightarrow P_2O_8^{4-} + 2e^- \quad \text{Eq. 5}$$

$$2HCO_3^- + 2\,{}^{\bullet}OH \rightarrow C_2O_6^{2-} + 2H_2O \quad \text{Eq. 6}$$

Peroxodiphosphates (Eq. 5) exhibit great stability at pH 12.5 but become highly reactive at significantly different values [14]. Although the action of these agents may contribute to the oxidation process, it is necessary to consider the conditions of their production (pH and temperature), in addition to the limitations in the mass transfer processes. Because of the difficulty of distinguishing between mediated oxidation and electrochemical incineration pathways during actual water treatment, the predominance of these reaction pathways was explored in this study using spectroelectrochemical (SEC) analyses with tert-butyl alcohol. This study aimed to provide a technological solution to the problem of handling wastewater effluent from the desalting process in industrial oil refining by employing BDD and/or alternative materials (dimensionally stable anodes, hereafter DSAs®).

2. EXPERIMENTAL

2.1. Chemicals

Sulfuric acid (H_2SO_4), hydrochloric acid (HCl), and phenol (C_6H_5OH) were obtained from JT Baker. Coumarin, 7-hydroxycoumarin, and tert-butyl alcohol were obtained from Aldrich.

2.2. Instruments

Polycrystalline BDD [(B) = 500–1300 ppm] film (Si/BDD) with a thickness of 2–3 μm was synthesized via hot filament chemical vapor deposition (HF-CVD) and was provided by Adamant Technologies. Electrolysis was performed in a conventional 2-electrode cell (130 mL) with a cooling jacket using a BK Precision XLN1001 power source. The stirring was performed using a magnetic

stirrer, and the temperature control was performed with a Prendo ECO-06 heat exchanger. The TOC analyses were performed using Shimadzu ASI-L equipment. The turbidity and suspended solids were evaluated using HACH DR/890 equipment. The color was analyzed using a HACH DR6000 colorimeter, and both the pH and electrical conductivity were measured using a BANTE Instruments Bante901 pH/conductivity meter. Analyses of the organic compounds in the actual sample, the synthetic phenol, and the decrease in the amount of coumarin (the probe compound used in $^{\bullet}OH$ analysis) with or without tert-butyl alcohol were performed in situ by coupling two techniques: visible ultraviolet spectroscopy and anodic polarization (spectroelectrochemical). The previous technique was performed using a Lambda XLS^{+} spectrophotometer, an Agilent flow cell, and a Masterflex® K/S pump, which were adapted to the electrolysis cell, whereas 7-hydroxycoumarin detection was performed using a Cary Eclipse Fluorescence Spectrophotometer from Agilent (Fig. 1). The potentially toxic elements (PTEs) were identified using a Perkin Elmer Optima 3300 DV model and a Perkin Elmer 200/MHS-15 Analyzer. The first instrument was used for inductively coupled plasma (ICP) analysis, and the second was employed for Hg analyses via hydride generation. Analysis of the volatile organic compounds (VOCs) was performed using an Agilent 7090A gas chromatograph coupled with a 5975 mass spectrometer, whereas the analysis of the semivolatile organic compounds (SVOCs) was performed using an Agilent 6890 Plus gas chromatograph coupled with a 5973N mass spectrometer. For the anion analysis, a Dionex ICS-2500 HPLC/IC high-performance liquid chromatograph with a conductivity detector (ED50A) was used.

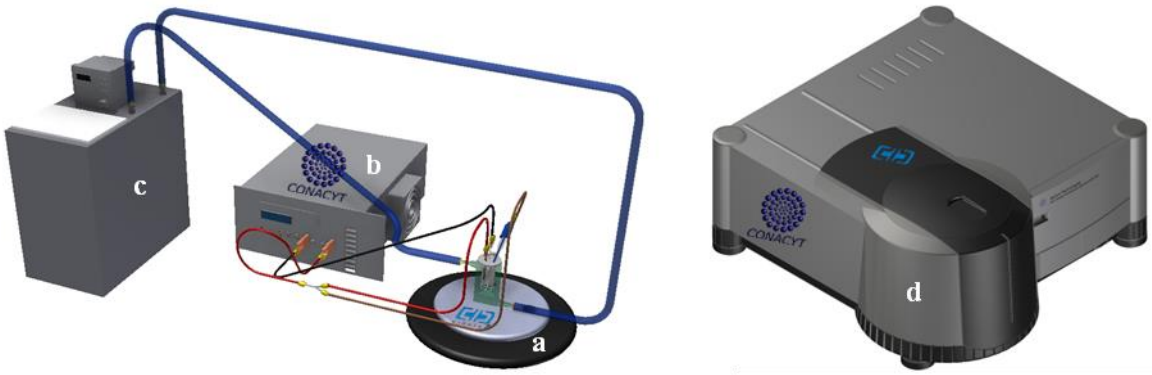

Figure 1. Experimental system for the SEC analyses: a) electrochemical cell, b) rectifier, c) heat exchange, and d) fluorimeter.

2.3. Analytical procedures

2.3.1. Characterization of the samples.

Sample preparation. For the different analyses, a composite sample was obtained from individual samples of the effluents from the crude oil desalting process. The effluents were treated in the sour water oxidation plant, where sulfides are removed. The effluents were sampled for 22 days, and each day 20 L (440 L in total) were obtained, mixed, and stored at 277.15 K. Immediately before a

sample was taken for the experimental tests and analyses, the container was vigorously shaken. Throughout the sample preparation process, a strict safety protocol was employed, which included the use of a customized infrastructure (with an extraction hood coupled to a gas scrubber), protective equipment (such as gas masks and nitrile and neoprene gloves), and special attire.

Physicochemical analysis. The cation analysis was performed using plasma emission spectrometry (ICP), except for Hg, which was analyzed via hydride generation-flame atomic-absorption spectrophotometry (HG-FAAS). The analysis was performed after digestion of the samples. The concentration of anions present was determined via ion chromatography according to EPA method 300.1 (EPA, 1997). A Dionex IonPac AS14A column with a flow rate of 1 mL min^{-1} was used, and Na_2CO_3/$NaHCO_3$ was used as the eluent. The equipment was calibrated using solutions prepared from Dionex's 7-Anion Standard, and the quality of the results was evaluated via comparison with the IC-FAS-1A certified standard from Inorganic Ventures. Other physicochemical analyses were performed using ASTM's standard procedures.

Volatile analysis. In this qualitative analysis, the sample was introduced into the chromatography system through an AtomX Teledyne Tekmar purge and tramp sample concentrator using the head space technique. A DB-624 column (dimensions 30 m x 0.32 mm, 1.8 μm) with a stationary phase of 5% phenyl-methyl-siloxane was used. The carrier gas was helium-grade UHP. The injection of the sample was performed in split mode 15:1, with a flow rate of 1.22 mL min^{-1}. The temperature of the injector was 473.15 K, and the initial oven temperature was 383.15 K, which was maintained for 5 min and then ramped at 281.15 K min^{-1}, until it reached a stable temperature of 513.15 K for 1 min, for a total time of 31 min.

Semivolatile analysis. The qualitative determination of SVOCs was performed using a gas chromatograph coupled to a mass spectrometer (GC-MS) according to EPA procedure 3550/EPA 8270. Before the analysis, the sample was homogenized and extracted with HPLC-grade dichloromethane after acidification to acid pH <2 and again at pH >11. Subsequently, both extracts (acids and alkalis) were mixed and concentrated with a Kuderna-Danish concentrator to a volume of 1 mL. An HP-5 MS column (dimensions 30 m x 0.25 mm, 0.25 μm) with a stationary phase of 5% phenyl-methyl-siloxane was used. The carrier gas was helium-grade UHP. The injection of the sample was performed in split mode 5:1 at a flow rate of 1.2 mL min^{-1}. The temperature of the injector was 543 K, with an initial oven temperature of 323 K (which was maintained for 4 min) and a ramp rate of 282 K per min, until a stable temperature of 573 K was sustained for 6 min, for a total time of 37.78 min.

2.3.2 Electrolysis of desalter effluent.

EOP (*electrochemical incineration/mediated oxidation*). Before performing the EOP, the Si/BDD electrode was activated using a specialized method [15]. The various electrolyses of water from the desalting process were performed in an undivided cell using geometrically active areas of 18.45 and 13.14 cm^2 for the anode and cathode [stainless steel 304 (SS-304)], respectively. The gap was 1 cm. The electrolyses were performed under agitation (6 rpm), and the temperature was

maintained at 298.15 K. The current density (j) values evaluated were 50, 100, and 150 mA cm^{-2}. To determine the optimal operating conditions, optimize resources, and avoid experimental errors related to sampling during electrolysis, the SEC technique was implemented. Thus, in situ monitoring of the degradation of aromatic compounds and reaction intermediates was performed in both the presence and absence of tert-butyl alcohol. The percentages of TOC removal were calculated according to the following formula (Eq. 7), where C_i is the initial concentration (mg L^{-1}) and C_f is the final concentration (mg L^{-1}).

$$\% \text{ removal} = C_i\text{-}C_f/C_i \times 100 \qquad \text{Eq. 7}$$

Additionally, in each experiment, representative samples were obtained at defined times for the physicochemical and chromatographic analyses.

$^{\bullet}$*OH analysis*. Analysis of the $^{\bullet}$OH produced on the surface of Si/BDD (Eq. 1) was performed using an SEC technique that monitored the decreased concentration of coumarin (probe compound) in situ. The $^{\bullet}$OH reacts with coumarin to form 7-hydroxycoumarin (Eq. 8), which can be measured via fluorescence spectroscopy. In the presence of tert-butyl alcohol, the action of $^{\bullet}$OH is inhibited.

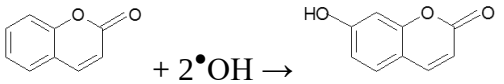

Eq. 8

Considering the possible presence of anions that can be electrolyzed (Cl^- and SO_4^{2-}) in real water, a mixture of coumarin with these anions was prepared in the laboratory and subjected to electrolysis with j values of 50 and 100 mA cm^{-2} for a reaction time (t_r) = 4 min.

3. RESULTS

3.1. Physicochemical analysis

Table 1 presents the results of the physicochemical characterization of the water from the desalting process (using the composite sample).

The amounts of fats and oils, BOD_5, and ammoniacal nitrogen (NH_3-N) exceeded the maximum permissible limits (MPL) for discharge into national resources specified in Mexican regulations (**NOM-001**). Additionally, the results revealed a high alkalinity, 549.70 mg L^{-1}, and a pH of 8.5, which reflects the reducing character of these effluents (some contaminants can be fixed at alkaline pH and be released under oxidizing conditions). However, the measured concentrations of phenol (4.68 mg L^{-1}), COD (1,706.87 mg L^{-1}), and dissolved solids (3,030 mg L^{-1}) were not comparable with any other type of effluent from the hydrocarbon industry [7]. Anion analysis via ion chromatography revealed chloride (Cl^-) and sulfate (SO_4^{-2}) contents of 1,235 and 164 mg L^{-1}, respectively. Although the presence of chlorides may lead to the formation of organochlorine compounds during electrolysis, it can also exert a synergistic effect on the electrochemical incineration

process by generating different oxidizing agents (acting within the bulk solution), which can destroy the organic compounds present (i.e., mediated oxidation). Both types of anions can significantly impact $^{\bullet}OH$ production during an EOP with BDD [7].

Table 1. Physicochemical analysis of the desalter effluent

Parameter	MPL (mg L^{-1}) in Rivers Protection of Aquatic Life (C)	
	p.d.**	p.m.**
Total phenol (mg L^{-1})	4.68	-	-
Oil and grease (mg L^{-1})	69.30	15	25
BOD_5 (mg L^{-1})	1,077	30	60
COD (mg O_2 L^{-1})	1,706.87	-	-
Sulfide reagents (mg L^{-1})	60.04	-	-
N-Nitrates (mg L^{-1})	<0.1035	-	-
NH_3-N	271.51	15	25
Cyanides (mg L^{-1})	<0.0217	-	-
pH*	8.50	-	-
TOC (mg L^{-1})	265.02	-	-
Conductivity (mS cm^{-1})	6,420	-	-
Alkalinity, $CaCO_3$ (mg L^{-1})	549.70	-	-
Total dissolved solid (mg L^{-1})	3,030	-	-
Settleable solids (mL L^{-1})	0.10	1	2
Total suspended solids (mg L^{-1})	40.00	40	60
F^- (mg L^{-1})	3.65	-	-
Cl^- (mg L^{-1})	1,235	-	-
Br^- (mg L^{-1})	<l.q.	-	-
NO_3^- (mg L^{-1})	1.01	-	-
NO_2^- (mg L^{-1})	<l.q.	-	-
PO_4^{3-} (mg L^{-1})	<l.q.	-	-
SO_4^{2-} (mg L^{-1})	164	-	-
ORP (mV)	-36.40	-	-
Turbidity (FTU)	320	-	-

MPL = Maximum permissible limits, p.d. = per day, p.m. = per month, l.q. = limit of quantification
*Values that exceed the established MPL under Mexican regulations.
**Average values.

Table 2 presents the different metals identified; note that high concentrations of calcium (Ca) and sodium (Na), 142.45 and 484.52 mg L^{-1}, respectively, were observed. These results are consistent with previously measured alkalinity values. PTEs such as As, Cd, Cr, Hg, and Ni remained below the limit of quantitation of the equipment, and the concentrations of Pb and Zn were less than the MPL (NOM-001).

Table 2. Analysis of PTEs in desalter effluent

PTEs (mg L^{-1})		MPL (mg L^{-1}) in Rivers					
		Agricultural Irrigation (A)		Public-Urban (B)		Protection of Aquatic Life (C)	
		p.d.*	p.m.*	p.d.*	p.m.*	p.d.*	p.m.*
Al	0.48	-	-	-	-	-	-
As	0.038	0.2	0.4	0.1	0.2	0.1	0.2
Cd	<0.06	0.2	0.4	0.1	0.2	0.1	0.2
Co	<0.063	-	-	-	-	-	-
Cu	<0.079	4.0	6.0	4.0	6.0	4.0	6.0
Cr	<0.049	1.0	1.5	0.5	1.0	0.5	1.0
Fe	0.450	-	-	-	-	-	-
Mn	0.131	-	-	-	-	-	-
Ca	142.45	-	-	-	-	-	-
Mg	22.92	-	-	-	-	-	-
Na	484.52	-	-	-	-	-	-
Hg	<0.000936	0.01	0.02	0.005	0.01	0.005	0.01
Ni	<0.047	2	4	2	4	2	4
Pb	0.115	0.5	1	0.2	0.4	0.2	0.4
Zn	0.186	10	20	10	10	20	10
V	0.120	-	-	-	-	-	-

MPL = Maximum permissible limits, p.d. = per day, p.m. = per month

*Average values

3.2 Analysis via GC-MS

A GC-MS analysis (of *VOCs* and *SVOCs*) for the desalter effluent mixture was conducted to qualitatively identify the nature of the different organic compounds present in the sample before and after the EOP. The results are shown in Table 3. Importantly, most of the identified compounds are highly toxic [6].

Table 3. GC-MS analysis of the desalter effluent

Organic Compounds	Before	After
Volatile	benzene, acetic acid, toluene, tetrahydro-thiophene, tetrahydro-2-methyl-thiophene, ethylbenzene, 1,3-dimethyl-benzene, o-xylene, 1-ethyl-4-methyl-benzene, 1,2,3-trimethyl-benzene, decane, 1-ethyl-4-methyl-benzene 1,2,3-trimethyl-benzene,	dichloronitro-ethane

	eucalyptol, 3-methyl-decane, 2-ethyl-1,4-dimethyl-benzene, undecane, dodecane, 1-methylene-1H-indene, tridecane, 1-methyl naphthalene, tetradecane, cyclotetradecane, pentadecane, hexadecane	
Semivolatile	methylbenzene (toluene), phenol, decane, 1,8-cineole, 2-methyl-phenol, 4-methyl-phenol, undecane, 2-ethyl-phenol, 2,4-dimethyl-phenol, 3-ethyl-phenol, 2,3-dimethyl-phenol, dodecane, endobornyl acetate, tridecane, 2,6,10-trimethyl-dodecane, tetradecane, pentatriacontane, pentadecane, hexadecane, heptadecane, 2,6,11,15-tetramethyl-hexadecane, octadecane, nonadecane, eicosane, molecular sulfur, heneicosane, docosane, 8-methyl-4-azafluorenone, tricosane, hexatriacontane, eicosane, pentatriacontane, tritetracontane.	toluene, tetrachloro-ethene, p-xylene, 1,3-dimethyl-benzene, 1,3,5,7-cyclooctatetraene styrene

3.3 Electrolysis

3.3.1 Selection of current density and reaction time

To select the main operating variables — such as j and t_r, which affect the EOP —for evaluating the different reaction pathways (electrochemical incineration and mediated oxidation), analyses were performed using acidic mediums to remove organic compounds (via spectroelectrochemistry), TOC, and $^{\bullet}OH$ (via fluorescence spectroscopy). Fig. 2a shows the characteristic absorption spectra obtained by applying a j = 100 mA cm^{-2} for t_r = 30 min at pH 3 (adjusted with concentrated H_2SO_4). The initial measurement revealed a peak at approximately 300 nm, which gradually decreased with time. Under the above operating conditions, similar profiles were obtained for both j = 50 and 150 mA cm^{-2}, and only the normalized values (λ = 300 nm) are shown in Fig. 2b. It was observed that after t_r = 25 min, when j was 100 or 150 mA cm^{-2}, the degradation of the organic compounds was similar, whereas the degradation was weaker when j = 50 mA cm^{-2}.

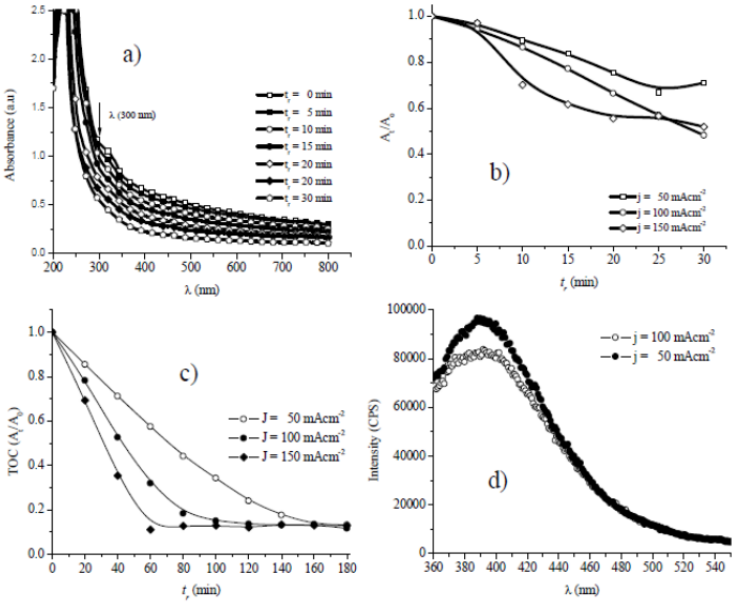

Figure 2. a) SEC analysis of the EOP using Si/BDD with j = 100 mA cm^{-2}. b) Normalization of the spectra obtained when evaluating j values of 50, 100, and 150 mA cm^{-2} (λ = 300 nm) at t_r = 30 min. c) TOC analysis at t_r = 180 min, conditions: 25°C, 6 rpm, pH = 3 (adjusted with concentrated H_2SO_4). d) $^{\bullet}$OH analysis, conditions: 0.1 mM coumarin, j = 50 and 100 mA cm^{-2}, 25°C, 6 rpm, supporting electrolyte (0.5 M HCl + 0.5 M H_2SO_4), t_r = 4 min.

To confirm the degree of mineralization obtained from each value of j (50, 100, and 150 mA cm^{-2}) at t_r = 30 min, the initial and final samples were analyzed by quantifying the TOC. The results indicated that 20.81, 28.09, and 46.64% of the TOC was removed when j was 50, 100, and 150 mA cm^{-2}, respectively. A j value of 100 mA cm^{-2} was preliminarily selected. To confirm the appropriate j and t_r values to achieve complete mineralization, the above experiments were repeated, and the analysis was performed only in terms of TOC for t_r = 180 min. Fig. 2c shows the normalized values of TOC (TOC_t/TOC_0). At t_r = 140 min, >90% removal was obtained for all three values of j. Based on this analysis and considering the current limit for $^{\bullet}$OH production [7] and the expected increase in energy expenditure resulting from employing j = 150 mA cm^{-2}, values of j = 100 mA cm^{-2} and t_r = 3 h were selected to perform the subsequent tests. Fig. 2d shows the results of the $^{\bullet}$OH analysis performed via fluorescence spectroscopy at j = 50 and 100 mA cm^{-2} and t_r = 4 min (0.5 M HCl + 0.5 M H_2SO_4). The spectra obtained with both values of j indicated the presence of 7-hydroxycoumarin, thus confirming the presence of $^{\bullet}$OH. When j = 50 mA cm^{-2}, a higher fluorescence intensity was observed than with j = 100 mA cm^{-2}, which indicated lower $^{\bullet}$OH production. Thus, as j was increased, there was more $^{\bullet}$OH production and faster consumption of both the coumarin and the reaction product, 7-hydroxycoumarin [16].

The above results are consistent with the TOC results and the tests performed using in situ UV-Vis spectroscopy. Additionally, this analysis confirms that the electrochemical incineration process (which occurs via $^{\bullet}$OH) is involved during the EOP in a medium containing SO_4^{2-} and Cl^-, anions commonly found in water from the crude oil desalting process (Table 1). Thus far, the results do not indicate the predominance of one reaction pathway; this will be demonstrated later. It is important to

note that during water oxidation with BDD (Eq. 1) in a medium containing SO_4^{2-} ions, $^{\bullet}OH$ can induce the generation of secondary species, such as H_2O_2 (Eqs. 9–11), O_3 (Eqs. 12–14), and peroxodisulfuric acid, $H_2S_2O_8$ (Eq. 15) [10].

$$2^{\bullet}OH \rightarrow H_2O_2 \quad \text{Eq. 9}$$

$$H_2O_2 \rightarrow O_{2\,(g)} + 2H^+ + 2e^- \quad \text{Eq. 10}$$

$$H_2O_2 + {}^{\bullet}OH \rightarrow O_{2\,(g)} + 2H_2O \quad \text{Eq. 11}$$

$$^{\bullet}OH \rightarrow {}^{\bullet}O + H^+ + e^- \quad \text{Eq. 12}$$

$$^{\bullet}O + O_2 \rightarrow O_{3\,(g)} \quad \text{Eq. 13}$$

$$2^{\bullet}O \rightarrow O_{2\,(g)} \quad \text{Eq. 14}$$

$$2H_2SO_4 + 2^{\bullet}OH \rightarrow H_2S_2O_8 + 2H_2O \quad \text{Eq. 15}$$

Thus, it is valid to assume that H_2O_2, O_3, and $H_2S_2O_8$ may participate in the degradation process in addition to $^{\bullet}OH$. However, such species are *only* formed in high quantities when there are mass transfer limitations. Therefore, it is assumed that $^{\bullet}OH$ is the main oxidizing agent among the mentioned species. In the same manner, the active chlorides (ClO^-, HClO, and Cl_2) can be oxidized to oxychlorine radicals, which can contribute to the oxidation process. The generation of these oxychlorine radicals and their participation in the oxidation process will be considered in the next section.

3.3.2 Effect of ionic composition and pH

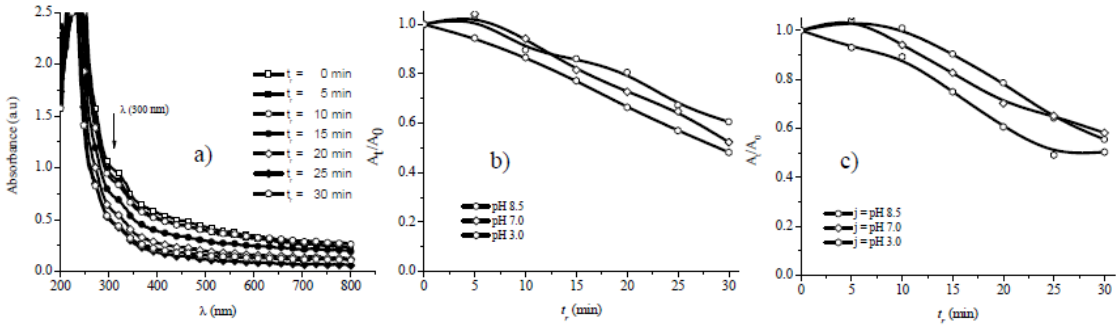

Figure 3. Spectroelectrochemical analysis of the desalted wastewater. Effect of the ionic composition: a) absorption spectra in the presence of tert-butyl alcohol (50 mM) at pH = 3 and j = 100 mA cm^{-2}, and normalized values (λ = 300 nm) at different pH values and SO_4^{2-} concentrations, b) in the absence of tert-butyl alcohol and c) in the presence of tert-butyl alcohol (50 mM); conditions: j = 100 mA cm^{-2}, 25°C, 6 rpm, t_r = 30 min. pH adjustments were performed using concentrated H_2SO_4.

Considering the presence of Cl^- and SO_4^{2-} at concentrations of 1,235 and 164 mg L^{-1}, respectively (Table 1), the effects of these anions on the oxidative process were also evaluated. Recently, we reported the great impact of ionic composition on $^{\bullet}OH$ production, in which production

was higher in a medium containing SO_4^{2-} [7]. Therefore, different electrolyses at natural pH (8.5) and pH values of 7 and 3 were performed to evaluate the effect of the concentration of SO_4^{2-} on the oxidative process. The pH was adjusted (to 7 and 3) via the addition of concentrated H_2SO_4. Fig. 3a shows the absorption spectrum obtained via spectroelectrochemistry when applying j = 100 mA cm^{-2} for t_r = 30 min at pH 3 in the presence of tert-butyl alcohol, a known $^{\bullet}OH$ scavenger (k = 6 x 10^8 $M^{-1}S^{-1}$) [17; 18; 19; 20].

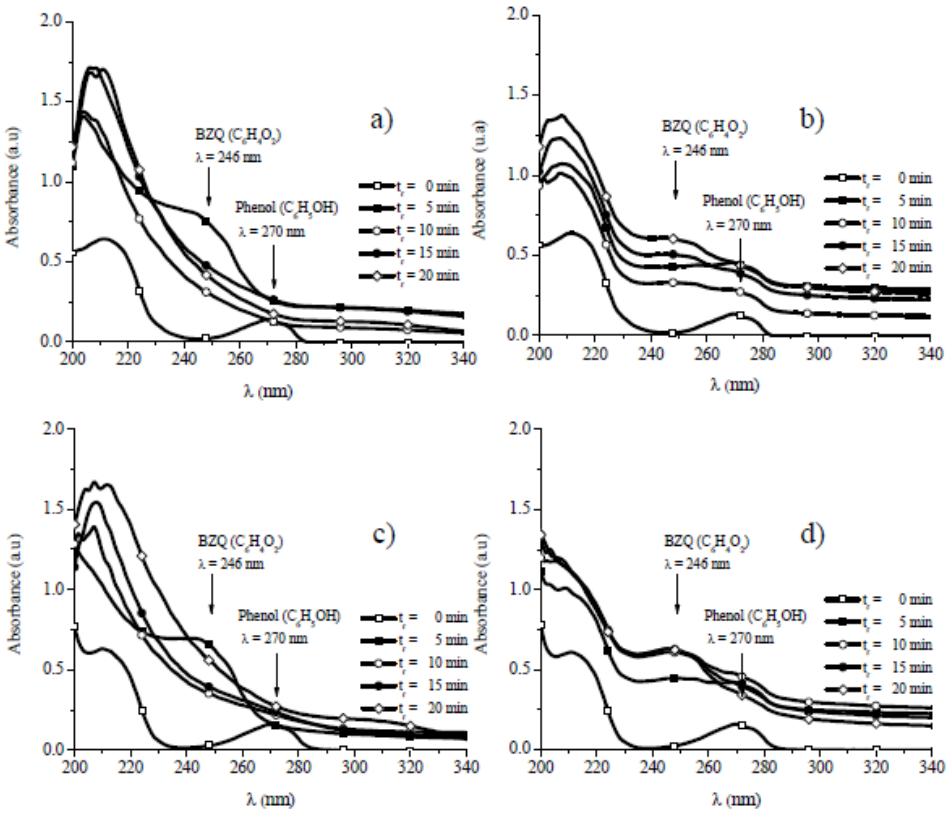

Figure 4. Absorption spectra obtained via spectroelectrochemistry of a synthetic phenol oxidation: a) 0.5 M H_2SO_4 + 15 mg L^{-1} phenol, b) 0.5 M H_2SO_4 + 15 mg L^{-1} phenol + 50 mM tert-butyl alcohol, c) 0.5 M H_2SO_4 + 0.1 mM KCl + 15 mg L^{-1} phenol and d) 0.5 M H_2SO_4 + 0.1 mM KCl + 15 mg L^{-1} phenol + 50 mM tert-butyl alcohol. Conditions: j = 100 mA cm^{-2}, 25°C, 6 rpm, t_r = 20 min.

The results indicated that the oxidative process followed the same trend as that observed in Fig. 2a in the absence of tert-butyl alcohol, i.e., no significant effect was observed when suppressing the involvement of $^{\bullet}OH$'s. The same effect was observed for the absorption spectra obtained at pH values of 7 and 8.5, and only the normalized absorbance values (A_t/A_o) obtained at λ = 300 nm are shown for the experiments performed in the absence (Fig. 3b) and presence (Fig. 3c) of tert-butyl alcohol. The absorption spectra of the experiment without tert-butyl alcohol gradually decreased during the oxidative process, as did those obtained in the presence of tert-butyl alcohol. In the absence of tert-butyl alcohol, the A_t/A_o (Fig. 3b) exhibited the following trend (t_r = 30 min): pH 3 > pH 7 > pH 8.5. At t_r = 30 min, the TOC analysis revealed removal efficiencies of 28.1, 13.4, and 14.4% for the

experiments with pH values of 3, 7, and 8.5, respectively, in the absence of tert-butyl alcohol. The TOC analysis in the presence of tert-butyl alcohol was not possible owing to the high carbon content present in this reagent. It is important to note that during the electrolysis, the smell of chlorine gas was extremely strong; therefore, the solution was handled under the extraction hood at all times. These vapors are expected due to the high amount of chlorides in the electrolyzed sample (1,235 mg L^{-1}). Eliminating the participation of $^{\bullet}OH$, it is valid to assume some participation by the active chlorine species (Cl_2, HOCl, and OCl). To confirm this assumption, a second test was performed. This test consisted of the preparation of *synthetic solutions* of phenol (15 mg L^{-1}) (a chemical species identified in the desalter effluent) in four different reaction media, i.e., in H_2SO_4 and H_2SO_4 + 0.1 mM KCl, with and without tert-butyl alcohol, to demonstrate their behavior during electrolysis. The experiments were performed under the following conditions: j = 100 mA cm^{-2}, 25°C, 6 rpm, and t_r = 20 min.

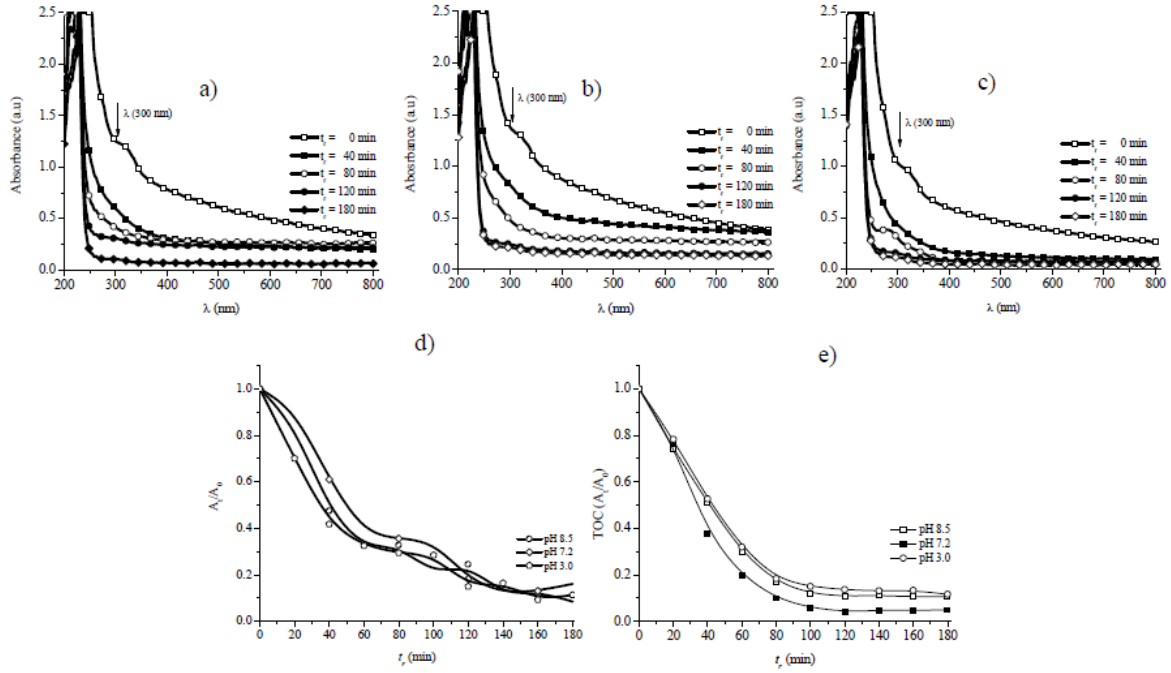

Figure 5. Effect of pH and t_r on the electrolysis of water from the crude oil desalting process using Si/BDD: a) pH = 8.5, b) pH = 7.2, c) pH = 3.02, d) normalized values A_t/A_o at λ = 300 nm, and e) normalized values of TOC_t/TOC_0. Conditions: j = 100 mA cm^{-2}, 25°C, 6 rpm, and t_r = 3 h. The pH adjustment was performed with concentrated H_2SO_4.

In a solution of 0.5 M H_2SO_4 without tert-butyl alcohol (Fig. 4a), the formation of benzoquinone (BZQ) (λ = 246 nm) increased at t_r = 5 min and then decreased. When tert-butyl alcohol was added to the same medium (Fig. 4b), this band decreased significantly. These changes in intensity were attributed to the scavenging of $^{\bullet}OH$. When the experiment was performed in H_2SO_4 + 0.1 mM KCl in the absence of tert-butyl alcohol (Fig. 4c), the amount of BZQ formed was similar to that observed in 0.5 M H_2SO_4 (Fig. 4a). However, in the presence of tert-butyl alcohol (Fig. 4d), no significant change was observed, indicating again the predominance of mediated oxidation. From the results obtained so far, we conclude that in a mixture containing sulfates and chlorides, although $^{\bullet}OH$'s

are produced, chlorides have the greatest oxidative power. Although the composition of the wastewater from the crude oil desalting process was altered by adding SO_4^{2-} ions (to produce a greater amount of $^{\bullet}OH$) in the experiments shown in Fig. 3b and c, the experiment was performed only at a t_r = 30 min. Therefore, to confirm the effect of pH and its relation to t_r, the best conditions, j = 100 mA cm^{-2}, were evaluated for the same pH values (8.5, 7, and 3) but at t_r = 3 h.

Figures 5a, b, and c show the profiles obtained via spectroelectrochemistry with natural (8.5), neutral (7.2), and acidic (3.0) pH values, respectively. The obtained spectra did not exhibit any significant differences, except for one corresponding to electrolysis at pH = 3 (Fig. 5c), where the band intensity (λ = 300 nm) was slightly less.

Table 4. Physicochemical characterization during the evaluation of pH effect and t_r. Conditions: j = 100 mA cm^{-2}, 25°C, 6 rpm, t_r = 3 h, and pH values of 8.5, 7.2, and 3.02.

		TOC (mg L^{-1})			Color (Pt-Co)			Total suspended solids (mg L^{-1})			Turbidity (FAU)			Conductivity (mScm^{-1})	
pH_i	pH_f	t_r = 0 h	t_r = 3 h	% removal	t_r = 0 h	t_r = 3 h	% removal	t_r = 0 h	t_r = 3 h	% removal	t_r = 0 h	t_r = 3 h	% removal	t_r = 0 h	t_r = 3 h
8.50	2.02	265.20	4.609	98.26	1594	4	99.74	222	0	100	286	10	96.50	5.454	2.54
7.20	2.04	265.20	4.728	98.21	1606	11	99.30	225	2	99.11	286	10	96.50	5.382	5.79
3.02	1.76	265.20	5.675	97.86	1212	10	99.17	168	1	99.40	216	10	97.22	5.722	11.71

Fig. 5d shows the normalized values (λ = 300 nm), which clearly show that the results for the different pH values obeyed the same trend up to t_r = 2 h, and then they all stabilized without any differences. To confirm the above results, a TOC analysis was performed. Fig. 5e shows the different TOC profiles as a function of the pH (normalized values, TOC_t/TOC_0). There was no significant long-term difference (t_r >2 h) between them, agreeing with the in situ SEC analysis.

Table 4 presents the results of the physicochemical characterization performed before and after the different electrolyses. The initial pH values of 8.5, 7.2, and 3.02 changed drastically after 2 min, reaching completely acidic values of 2.02, 2.04, and 1.76, respectively.

The drastic decrease in pH in each experiment explains the fact that the profiles obtained via spectroelectrochemistry, like the TOC profiles, were similar. This is congruent with a high amount of H^+, which is associated with the formation of HClO, a species with greater oxidizing capacity than ClO^- [21]. The rapid formation of hypochlorous acid explains why degradation occurred even at initial pH values of 8.5 and 7. Considering that in the initial characterization (Table 1) phenols, reactive sulfides, and hydrocarbons were detected, a decrease in the pH would lead to the release of highly toxic substances [7]. The hypothesis presented in the present study regarding the action of active chlorine (ClO^-, HClO, and Cl_2) and suppression of the action of $^{\bullet}OH$ does not exclude the participation of other species, such as oxychlorine radicals ($ClO^{\bullet}$, $ClO_2^{\bullet}$, $Cl^{\bullet}$, and $HOCl^{\bullet}$) and oxychlorine anion

radicals ($Cl_2^{\bullet-}$ and $HOCl^{\bullet-}$) [22]. The above claim is supported by noting that at initial pH values of 8.5 and 7.0, Si/BDD has a low η–O_2, which inhibits the formation of $^{\bullet}OH$. It has been reported that in NaOH (pH 12), $^{\bullet}OH$ is not generated via OH^- oxidation [23]. Moreover, in neutral-to-alkaline media, inorganic carbon can scavenge $^{\bullet}OH$ (Eq. 16) [24].

$$^{\bullet}OH + CO_3^{2-} \rightarrow OH^- + CO^{3-} \quad \text{Eq. 16}$$

Therefore, the initial pH values (8.5 and 7.0) could only have an initial effect (t_r = 0–2 min) on the production of ClO^-, whereas at t_r = 2–180 min, both HClO and $Cl_{2\,(g)}$, which were the predominant species, favored mediated oxidation over electrochemical incineration.

4. CONCLUSIONS

Wastewater from the crude oil desalting process was successfully treated via electrochemical oxidation using a Si/BDD anode. Under the optimal operating conditions (natural pH, j = 100 mA cm^{-2}, and t_r = 3 h), the predominant oxidizing species formed was HClO. In electrolysis at pH values of 7 and 3, the same behavior as at natural pH was observed; thus, the effect of varying the pH was insignificant. In all the experiments (regardless of the pH), the solution was rapidly acidified (in 2 min) to a pH value of 2.05. The $^{\bullet}OH$s generated at the BDD anode oxidized HClO to form oxychloride radicals. Using a $^{\bullet}OH$ scavenger, tert-butyl alcohol, it was demonstrated that the oxidation reactions of the hydrocarbons and phenolics had the same removal efficiency regardless of whether the $^{\bullet}OH$ participated. Therefore, it was concluded that the oxidation process was mediated by HClO.

ACKNOWLEDGMENTS
The authors would like to thank Mexico's National Council of Science and Technology (CONACyT) and PEMEX for their financial support of this research.

References

1. A. Pak and T. Mohammadi, *Desalination* 222 (2008) 249.
2. E. Aryafard, M. Farsi, M.R. Rahimpour and S. Raeissi, *J. Taiwan Inst. Chem. Eng.* 58 (2016) 141.
3. S. Norouzbahari, R. Roostaazad and M. Hesampour, *Desalination* 238 (2009) 174.
4. S. Dadari, M. Rahimi and S. Zinadini, *Desalination* 377 (2016) 34.
5. Z.-S. Bai and H.-L. Wang, *Chem. Eng. Res. Des.* 85 (2007) 1586.
6. A. Medel, E. Bustos, K. Esquivel, L.A. Godínez and Y. Meas, *Int. J. Photoenergy* 2012 (2012) 1.
7. A. Medel, E. Méndez, J.L. Hernández-López, J.A. Ramírez, J. Cárdenas, R.F. Frausto, L.A. Godínez, E. Bustos and Y. Meas, *Int. J. Photoenergy* 2015 (2015) .
8. Ch. Comninellis, *Electrochim. Acta* 39 (1994) 1857–1862.

9. B. Marselli, J. Garcia-Gomez, P.-A. Michaud, M.A. Rodrigo and Ch. Comninellis, *J. Electrochem. Soc.* 150 (2003) D79.
10. P-A. Michaud, M. Panizza, L. Ouattara, T. Diaco, G. Foti and Ch. Comninellis, *J. Appl. Electrochem.* 33 (2003) 151.
11. A. Kraft, M. Stadelmann and M. Blaschke, *J. Hazard. Mater.* B103 (2003) 247.
12. M. Panizza and G. Cerisola, *Chem. Rev.* 109 (2009) 6541.
13. E.J. Ruiz, Y. Meas, R. Ortega-Borges and J.L. Jurado-Baizabal, *Surf. Eng. Appl. Electrochem.* 50 (2014), 478.
14. A. Sánchez, J. Llanos, C. Sáez, P. Cañizares and M.A. Rodrigo, *Chem. Eng. J.* 233 (2013) 8.
15. A. Medel, E. Bustos, L.M. Apátiga and Y. Meas, *Electrocatalysis* 4 (2013) 189.
16. D. Bejan, E. Guinea and N.J. Bunce, *Electrochim. Acta* 69 (2012) 275.
17. B. De Witte, J. Dewulf, K. Demeestere and H. Van Langenhove, *J. Hazard. Mater.* 161 (2009) 701.
18. J. Muff, L.R. Bennedsen and E.G. Søgaard, *J. Appl. Electrochem.* 41 (2011) 599.
19. J. Jeong, C. Kim and J. Yoon, *Water Res.* 43 (2009) 895.
20. M.E. Simonsen, J. Muff, L.R. Bennedsen, K.P. Kowalski, and E.G. Søgaard, *J. Photochem. Photobiol., A: Chem.* 216 (2010) 244.
21. J. Hao, S. Qiu, H. Li, T. Chen, H. Liu and L. Li, *Int. J. Food Microbiol.* 155 (2012) 99.
22. M. Murugananthan, S.S. Latha, G. B. Raju and S. Yoshihara, *Sep. Purif. Technol.* 79 (2011) 56.
23. S. García-Segura, F. Centellas and E. Brillas, *J. Phys. Chem. C* 116 (2012) 15500.
24. D. Wu, M. Liu, D. Dong and X. Zhou, *Microchem. J.* 85 (2007) 250.